Active control of acoustic reflection, absorption, and transmission using thin panel speakers

H. Zhu, R. Rajamani,[a] and K. A. Stelson
Department of Mechanical Engineering, University of Minnesota, Minneapolis, Minnesota 55455

(Received 3 October 2001; revised 27 October 2002; accepted 6 November 2002)

This paper explores the development of thin panels that can be controlled electronically so as to provide surfaces with desired reflection coefficients. Such panels can be used as either perfect reflectors or absorbers. They can also be designed to be transmission blockers that block the propagation of sound. The development of the control system is based on the use of wave separation algorithms that separate incident sound from reflected sound. In order to obtain a desired reflection coefficient, the reflected sound is controlled to appropriate levels. The incident sound is used as an acoustic reference for feedforward control and has the important property of being isolated from the action of the control system speaker. In order to use a panel as a transmission blocker, the acoustic pressure behind the panel is driven to zero. The use of the incident signal as a reference again plays a key role in successfully reducing broadband transmission of sound. The panels themselves are constructed using poster board and small rare-earth actuators. Detailed experimental results are presented showing the efficacy of the algorithms in achieving real-time control of reflection or transmission. The panels are able to effectively block transmission of broadband sound. Practical applications for these panels include enclosures for noisy machinery, noise-absorbing wallpaper, the development of sound walls, and the development of noise-blocking glass windows. [DOI: 10.1121/1.1534834]

PACS numbers: 43.50.Ki, 43.50.Jh, 43.20.El [MRS]

I. INTRODUCTION

Active noise cancellation (ANC) is achieved by introducing a canceling ''antinoise'' wave of equal amplitude and opposite phase using a secondary source. A review of ANC developments can be found in Hansen (1991) and Kuo and Morgan (1999). Lueg (1936) first suggested the idea of active noise cancellation. Early work on ANC used analog techniques. Chaplin (1977) introduced digital techniques in his ANC patent. Since then, much work on ANC using digital-processing techniques has been published. Adaptive feedforward control is the most popular and successful approach used in ANC (Kuo and Morgan, 1996). Feedforward control involves feeding a signal related to the disturbance input (called the primary noise) into the controller which then generates a signal to drive a speaker in such a way as to cancel the disturbance. This signal related to the primary noise is called the reference signal.

Results on many successful feedforward ANC systems have been published. However, the major limitations of ANC systems must be noted. First, most ANC systems need a reference signal. In the absence of a nonacoustic reference signal (such as from a speed sensor), reference microphones can be used to pick up signals from the primary source before the noise propagates to the secondary source. However, this leads to the ''secondary source effect.'' The reference microphones will not only pick up signals from the primary source but also those from the secondary source. A second limitation is that a high coherence between the reference microphone and the primary source is needed to achieve good performance. An additional complication is that online secondary path (from secondary source to the error microphone) estimation is needed to achieve long-term performance due to the nonstationary nature of ANC systems. However, it is difficult to estimate the secondary path online since random signals need to be used to excite the system and this tends to degrade the performance. Even if all of the above limitations could be addressed, it would still only be relatively easy to cancel noise at a point, i.e., at the position of the error microphone. It is very difficult for an ANC system to achieve global noise cancellation in a 3D environment such as in an enclosure. This is especially due to the limitations in the number of speakers and microphones that can be used in practical applications. This current research aims to address some of these limitations of ANC.

In this paper, we concentrate on the development of thin panels which can be electronically controlled so as to achieve desired acoustic properties. We develop algorithms for controlling the reflection coefficients of such panels as well as for using these panels as noise transmission blockers. The advantages of this approach to active noise control are that such panels can be used to prevent the entry of noise or the creation of noise, rather than the control of noise by active cancellation after it has already entered an enclosure. For example, panels made of glass can be used as window panes to prevent the entry of sound through windows in houses close to airports. Similarly, panels can be used to develop an enclosure for noisy machinery so as to prevent propagation of noise from the machinery. Such panels can also be used as wallpaper in rooms with noisy machinery so

[a]Electronic mail: rajamani@me.umn.edu, tel: (612) 626-7961, fax: (612) 624-1398.

as to prevent acoustic reflection and the occurrence of standing waves in the room.

The control system developed in this paper utilizes the separation of sound at a point into incident and reflected waves. The earliest work related to separation of reflected and incident sound is found in Guicking and Karcher (1984). They used two microphones and analog electronics consisting of four subtractions and four delays to obtain the incident wave and the reflected wave. They then attempted control of the reflected wave by appropriately setting the phase and gain of an amplifier.

The body of work closest to our approach is the research on active impedance control conducted by several researchers. Acoustic impedance at a surface is defined by

$$Z = \frac{p}{u}. \tag{1}$$

The acoustic impedance of air is $Z_o = 1/\rho_o c$, where ρ_o is the density of air and c is the speed of sound in air. By controlling the impedance at a surface to be equal to that of air, the reflection coefficient of the surface can be made zero if normal incidence is considered. A few researchers have studied this approach to active impedance control. Mehta *et al.* (1998) designed active acoustic treatment (AAT) cells using feedback control. Each cell included a microphone, a speaker, and an absorption sheet. They then used many cells aligned with the topside of a duct to attempt to attenuate sound transmission through a duct. Their objective was to obtain a perfect sound absorber.

A research group in France has been very active in the area of impedance control. In 1994, Thenail *et al.* studied how to actively increase the absorbent properties of a porous material. They found that the absorption is maximum when the space between the porous material and a rigid boundary is maintained at odd multiples of one quarter of the wavelength, and that driving the pressure at the back of an optimized porous material to zero will give maximum absorption. The latter finding is later used by them to implement indirect impedance control (Furstoss *et al.*, 1997). As for direct impedance control, Furstoss *et al.* (1997) used an accelerometer to measure velocity directly and a microphone to measure pressure. Thus, measuring impedance directly, they then control the impedance in a duct to simulate wall impedance control (Thenail *et al.*, 1997). They also used these two methods to actively control the sound field in a cavity via wall impedance control (Lacour *et al.*, 2000). Both one-dimensional cavities and three-dimensional cavities were investigated. Other related research has been conducted by Henrioulle *et al.* (1999), who designed a 1/4-wavelength absorber. This idea is similar to the work of Thenail *et al.* (1994). However, an important difference is that they used a flat speaker as a control actuator, which saves space (Henrioulle *et al.*, 1999). All of the above noted researchers aimed to control the absorption indirectly with the help of absorbing material, while the approach presented in this paper controls the sound reflection directly without absorbing material.

As far as control of sound transmission through a wall or a panel, very few studies have been conducted. Paurobally *et al.* (1999) investigated the use of feedback control to attenuate sound transmission through a double-panel partition (DPP). In their preliminary research, they reported a single-channel system with the secondary source being placed in the partition and pure tones being used to test the control system. The research related to DPP is different from the current research presented in this paper. In this paper, the panel itself plays both the role of sound entrance and the role of secondary source.

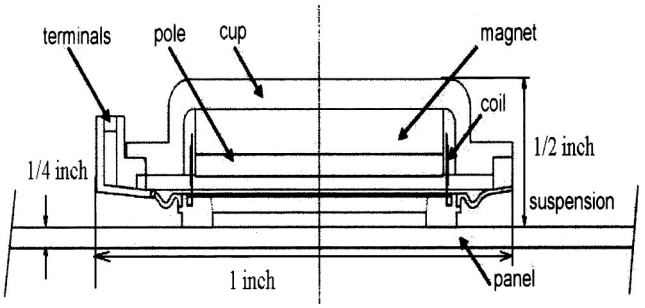

FIG. 1. NXT driver for a flat panel speaker.

The contributions of the present paper are the development of algorithms to enable control of the acoustic reflection coefficient or enable the prevention of noise transmission through the panel. The novelty of our approach is that the system developed in the paper is based purely on the use of microphones as sensors and that an algorithm to avoid the influence of the secondary source on the reference microphone is developed. The paper includes detailed experimental results documenting the performance of the both the reflection control systems and the ''transmission blocker'' systems.

II. FLAT PANEL ACTUATORS

We seek to use thin panels as speakers or actuators in our research. While a variety of exciter technologies can be considered for energizing the panel, including piezoelectric transducers, we chose a moving coil electromagnetic motor manufactured by Kodel, Inc. The use of a moving coil exciter ensures compatibility with conventional amplifiers. The exciter has a suspension which is glued to the desired panel. It also has terminals through which it can be connected to an amplifier. Allowable panels with this exciter include thin (about 6 mm) solid panels whose surface areas can range from several meters square to several centimeters square. The panels are different from conventional woofer speakers which operate under the ''pistonic'' mode of operation. Instead, they operate under a ''distributed mode'' in which the panel vibrates flexibly. The exciter is based on a technology developed by NXT (New Transducers Ltd.) under the principle of ''optimally distributed modes of vibration.'' Figure 1 shows a typical panel speaker consisting of both the panel and the exciter.

The typical response of the dynamics of a panel speaker (distributed modes loudspeaker, DML) is shown below in Fig. 2 and compared to that of a conventional cone speaker. It can be seen that the frequency response has many local valleys and peaks and does not offer the kind of flat response that would be ideal for feedback control. However, the dy-

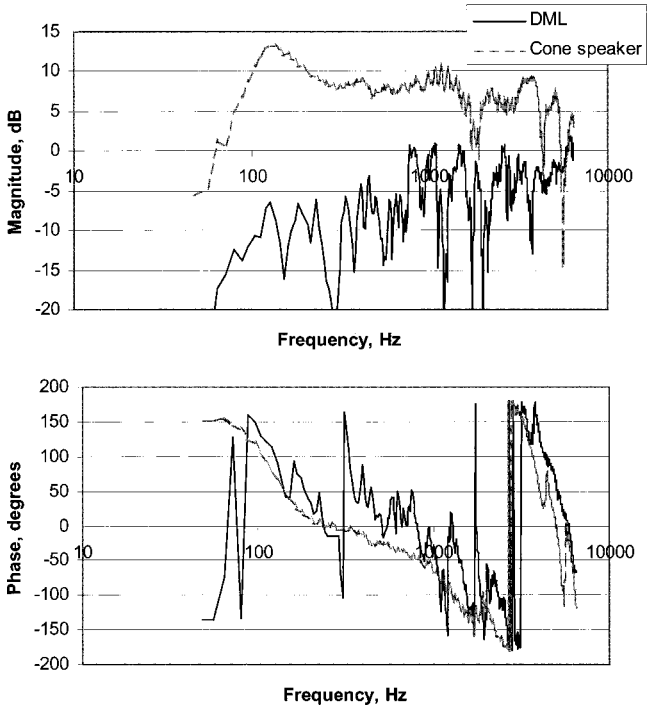

FIG. 2. Frequency response of DML and 8 in. standard cone speaker.

namics has been found to be consistent and repeatable. Feedforward control has been successfully implemented using these panels. Future research to optimize panel parameters such as size, panel material, internal damping, and exciter position for each application will be useful.

III. ACTIVE CONTROL OF REFLECTION COEFFICIENT

This section develops algorithms for separation of sound at the panel into incident and reflected signals and a control system that utilizes these signals for control of the reflection coefficient.

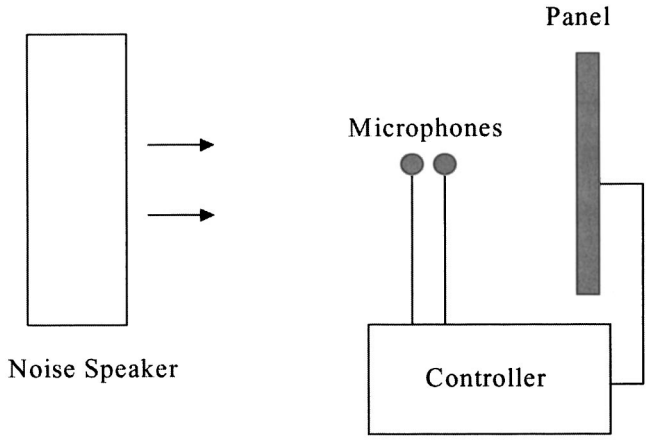

FIG. 3. Panel configuration for reflection control.

A. Wave separation using the integration method

The experimental system utilizes two microphones placed a few centimeters apart in front of the panel, as shown in Fig. 3. Normal incidence on the panel is assumed.

Let the acoustic pressure signals picked up by the two microphones be p_1 and p_2. If the distance d between the microphones is small relative to the smallest wavelength of the sound, the pressure at the midpoint is approximately

$$p=\frac{p_1+p_2}{2}. \tag{2}$$

For a plane wave, the momentum equation yields

$$\rho\frac{\partial u}{\partial t}+\frac{\partial p}{\partial x}=0. \tag{3}$$

Since the distance between the two microphones is small, the spatial derivative can be approximated by

$$\frac{\partial p}{\partial x}=\frac{p_2-p_1}{d}. \tag{4}$$

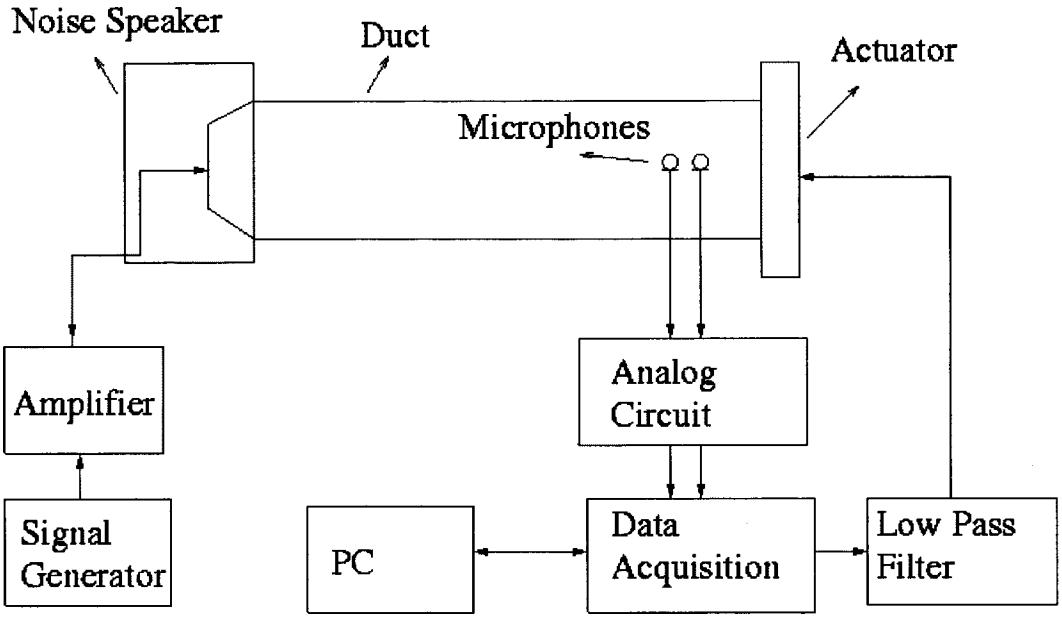

FIG. 4. Experimental setup for reflection coefficient control.

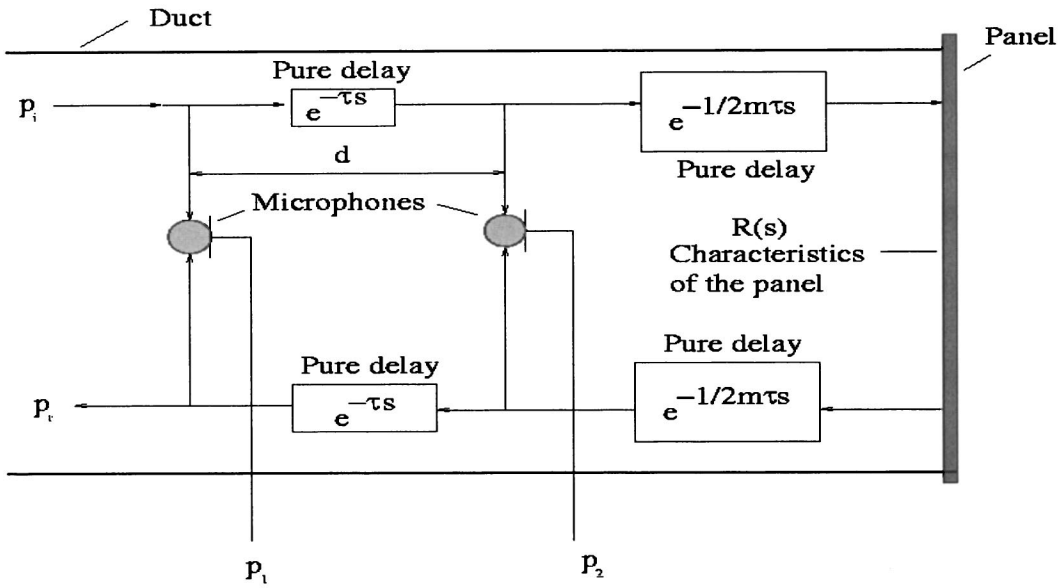

FIG. 5. The delay method for wave separation.

Substituting into Eq. (3), the particle velocity is calculated as

$$u(t)=\frac{1}{\rho d}\int_0^t (p_1-p_2)dx. \tag{5}$$

The incident wave can be expressed as (Beranek, 1954)

$$p_i=\sum_n A_n e^{j(w_n t-k_n x)}, \tag{6}$$

where the wave number k_n is related to the frequency ω_n and the speed of sound c by the relation $k_n=\omega_n/c$.

Substituting into the momentum Eq. (3), the particle velocity corresponding to the incident wave is

$$u_i=\frac{1}{\rho_0 c}p_i. \tag{7}$$

Similarly the particle velocity caused by the reflected wave can be obtained as

$$u_r=\frac{1}{\rho_0 c}p_r. \tag{8}$$

Thus, the overall particle velocity at the midpoint of the two microphones can be expressed as

$$u=u_i+u_r=\frac{1}{\rho_0 c}(p_i-p_r). \tag{9}$$

The associated pressure at the midpoint is

$$p=p_i+p_r. \tag{10}$$

Combining Eqs. (9) and (10), the incident wave and the reflected wave can be calculated by

$$p_i=\tfrac{1}{2}(p+\rho_0 c u), \tag{11}$$

and

$$p_r=\tfrac{1}{2}(p-\rho_0 c u). \tag{12}$$

To calculate p_i and p_r, p_1 and p_2 are first measured by the two closely positioned microphones. p is calculated using Eq. (2). Numerical integration is then used to update the particle velocity u, as shown in Eq. (5). Finally, Eqs. (11) and (12) are used to obtain p_i and p_r.

B. Active control of absorption or reflection

The experimental setup for control of the reflection coefficient is shown in Fig. 4. In the experiments, the primary noise is generated by a woofer speaker driven by a signal from a PC equipped with a data acquisition system. A 2-meter-long duct is used to isolate the environmental effects and ensure plane waves. The cross section of the duct is 17 by 17 cm. Thus, its cutoff frequency is about 1000 Hz. Two microphones, as described earlier, are used to measure acoustic pressure. The analog circuit provides functions of amplification and filtering. A CIO-DAS6402/12 data acquisition board is used to support data communication between PC and speakers and microphones. The control algorithm is implemented via a PC real-time toolbox with TURBO C used to develop the real-time code.

Assume that the desired reflection coefficient is a transfer function $R(s)$ that is the Laplace transform of the ratio

$$r=\frac{p_r}{p_i}. \tag{13}$$

The desired transfer function of the reflected wave is

$$P_{\text{rdes}}(s)=R(s)P_i(s), \tag{14}$$

and the corresponding desired reflected wave $p_{\text{rdes}}(t)$ can be calculated from

$$p_{\text{rdes}}(t)=\int_0^t p_i(t-\tau)r(\tau)d\tau. \tag{15}$$

The error p_r-p_{rdes} is used as the residue for feedforward control. The incident sound $p_i(t)$ is used as the reference signal. The secondary path transfer function is obtained from

$$S(s)=P_r(s)-R(s)P_i(s). \tag{16}$$

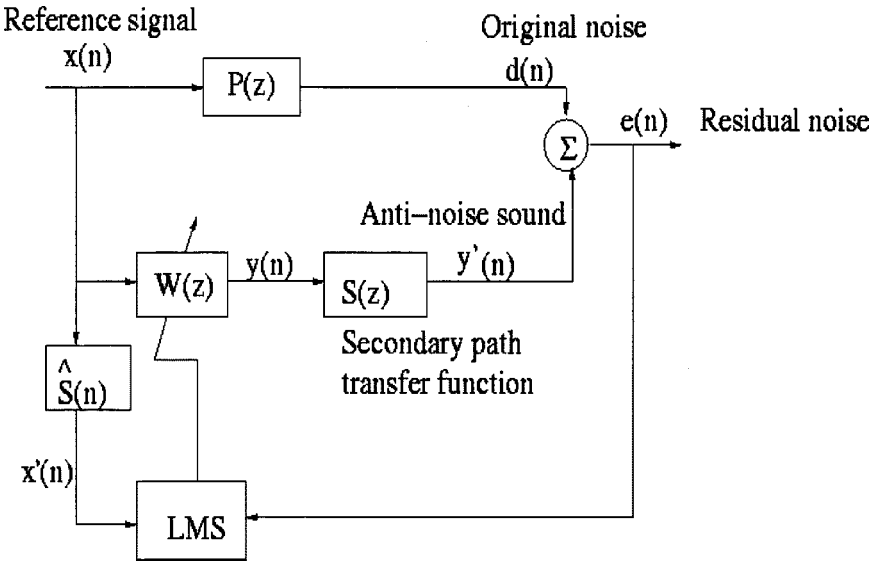

FIG. 6. FXLMS feedforward control.

Compared to the case where the error is the residual noise measured by a microphone, here the secondary path transfer function is not physically measured but is conceptual and has to be calculated from measurements. Using the incident sound as a reference signal ensures that the effect of the secondary source on the reference signal is avoided. Reflection can be controlled to obtain any desired reflection coefficient including $r=0$ (i.e., perfect absorption) and $r=1$ (perfect reflection).

C. Wave separation using the delay method

In the integration method, numerical integration must be used, slowing down the processing. In this section a different approach, the delay method, is proposed. The experimental setup is the same as shown in Fig. 4. Figure 5 is used to illustrate the idea.

As can be seen in Fig. 5, the signals p_1 and p_2 can be separated into two parts: incident wave and reflected wave. For a plane wave, the difference between the p_{1_i} and p_{2_r} is a pure time delay. Likewise, the difference between p_{2_r} and p_{1_r} is a pure time delay. The difference between p_{2_i} and p_{2_r} is another time delay multiplied by $R(s)$. If the delay between the microphones is τ, then $m=2\ell/d$, where ℓ is the distance between the second microphone and the actuator. Considering these relationships, we get

$$\frac{P_1(s)}{P_i(s)}=1+R(s)e^{-(m+2)\tau s}, \tag{17}$$

and

$$\frac{P_2(s)}{P_i(s)}=e^{-\tau s}+R(s)e^{-(m+1)\tau s}. \tag{18}$$

Let

$$x(t)=p_2(t)-p_1(t-\tau), \tag{19}$$

and

$$y(t)=p_1(t)-p_2(t-\tau). \tag{20}$$

We have

$$\frac{X(s)}{P_i(s)}=R(s)e^{-(m+1)\tau s}(1-e^{-2\tau s}), \tag{21}$$

and

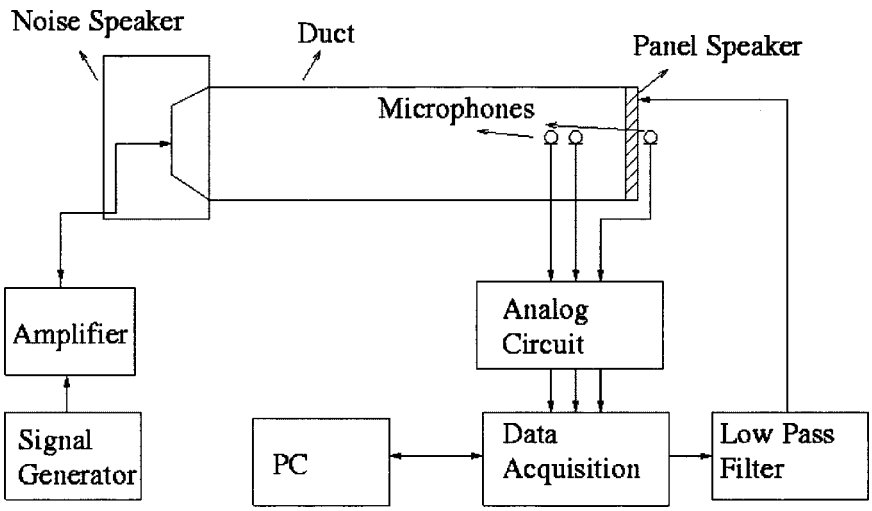

FIG. 7. Experimental setup for transmission control.

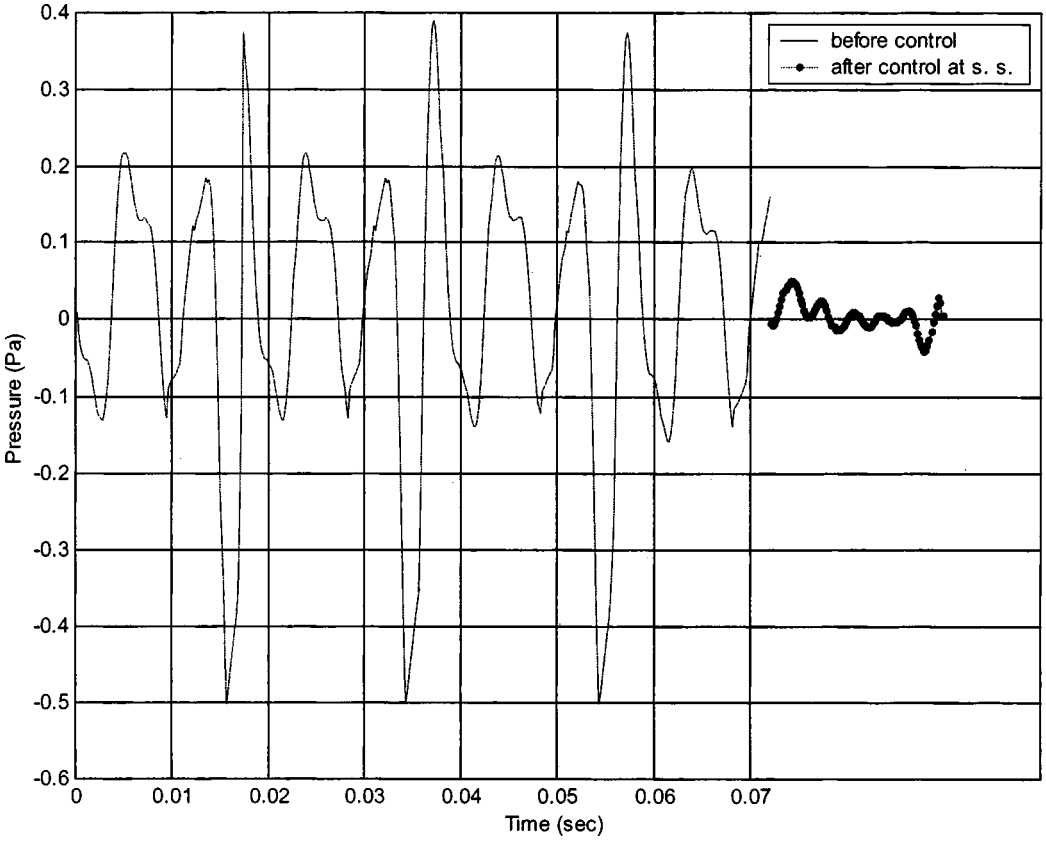

FIG. 8. Reflection control to achieve perfect absorption via integration method (primary noise consists of frequency components 150, 200, 250, and 300 Hz).

$$\frac{Y(s)}{P_i(s)} = (1 - e^{-2\tau s}). \tag{22}$$

Combining the above two equations gives

$$\frac{X(s)}{Y(s)} = R(s)e^{-(m+1)\tau s}. \tag{23}$$

Thus, in the delay method for wave separation, only delayed signals of p_1 and p_2 are used. x is controlled rather than p_r to obtain desired absorption/reflection. This method of wave separation is similar to the method presented in Guicking and Karcher (1984).

After the desired reflection coefficient transfer function, is determined, the desired transfer function of x can be found as

$$X_{\text{des}}(s) = Y(s)R_{\text{des}}(s)e^{-(m+1)\tau s}, \tag{24}$$

and the corresponding desired $x_{\text{des}}(t)$ can be calculated by the inverse Laplace transform

$$x_{\text{des}}(t) = L^{-1}(X(s)). \tag{25}$$

The error $x(t) - x_{\text{des}}(t)$ is used as the residue for feedforward control. The secondary path transfer function for feedforward control is

$$S(s) = X(s) - Y(s)R_{\text{des}}(s)e^{-(m+1)\tau s}. \tag{26}$$

Again, compared to the case where error is the residual noise measured by a microphone, here the secondary path transfer function is not physically measured but is conceptual and must be calculated from measurements. The algorithm obtained is thus quite simple with no integration required. However, an incident wave that can be used as a reference signal is not explicitly generated [instead the signals $x(t)$ and $y(t)$ are generated both of which contain information from both the incident and reflected wave]. The signal picked up by one of the microphones or $y(t)$ has to be used as the reference and the performance is therefore expected to degrade in the absence of a nonacoustic reference signal.

D. Filtered-x LMS algorithm

In the active control of reflection or absorption, the filtered-x least-mean-square (FXLMS) algorithm is used for the feedforward control. Figure 6 summarizes the popular FXLMS algorithm (Kuo and Morgan, 1996).

Here, $x(n)$ is the reference signal; $y(n)$ is the desired control (speaker) signal; $y'(n)$ is the actual sound of the secondary source; $d(n)$ is the undesired primary noise; $e(n)$ is the residual noise at downstream measured by an error microphone; $x'(n)$ is the filtered version of $x(n)$; $P(z)$ is the unknown transfer function between the reference microphone and the secondary source; $S(z)$ is the dynamics from the secondary source to the error microphone; $\hat{S}(z)$ is the estimation of this secondary path; and $W(z)$ is the digital filter that is adapted to generate the correct control signals to the secondary source. The objective is to minimize $e(n)$ via minimizing the instantaneous squared error, $\hat{\xi}(n) = e^2(n)$. The most widely used method to achieve this is the FXLMS algorithm, which updates the coefficients of $W(z)$ in the negative gradient direction with appropriate step size μ

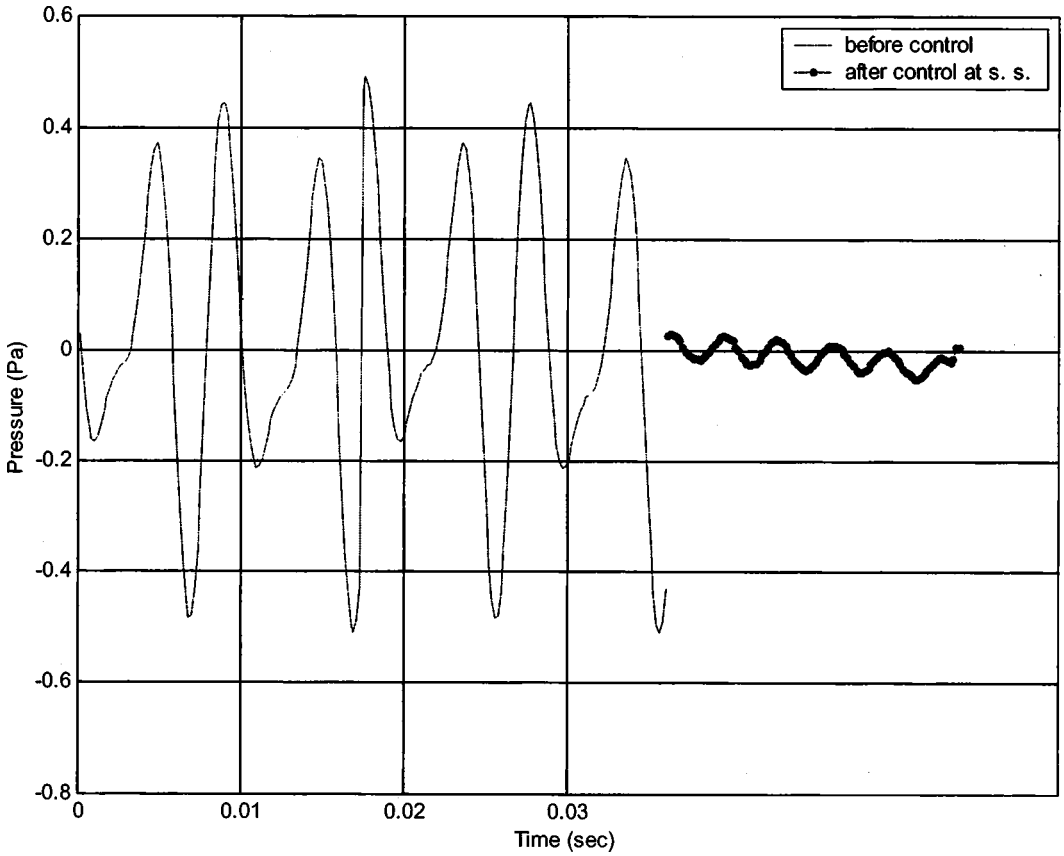

FIG. 9. Reflection control to achieve perfect absorption via integration method (primary noise consists of frequency components 100 and 300 Hz).

$$\mathbf{w}(n+1)=\mathbf{w}(n)-\frac{\mu}{2}\nabla\hat{\xi}(n), \tag{27}$$

where $\nabla\hat{\xi}(n)$ is the instantaneous estimate of the mean-square error gradient at time n, and can be expressed as

$$\begin{aligned}\nabla\hat{\xi}(n)&=2[\nabla e(n)]e(n)\\&=2[s(n)*x(n)]e(n)=2x'(n)e(n).\end{aligned} \tag{28}$$

By substituting the above equation back into (27), we have the filtered-x least-mean-square (FXLMS) algorithm

$$\mathbf{w}(n+1)=\mathbf{w}(n)+\mu x'(n)e(n), \tag{29}$$

where $x'(n)$ is estimated as $\hat{s}(n)*x(n)$.

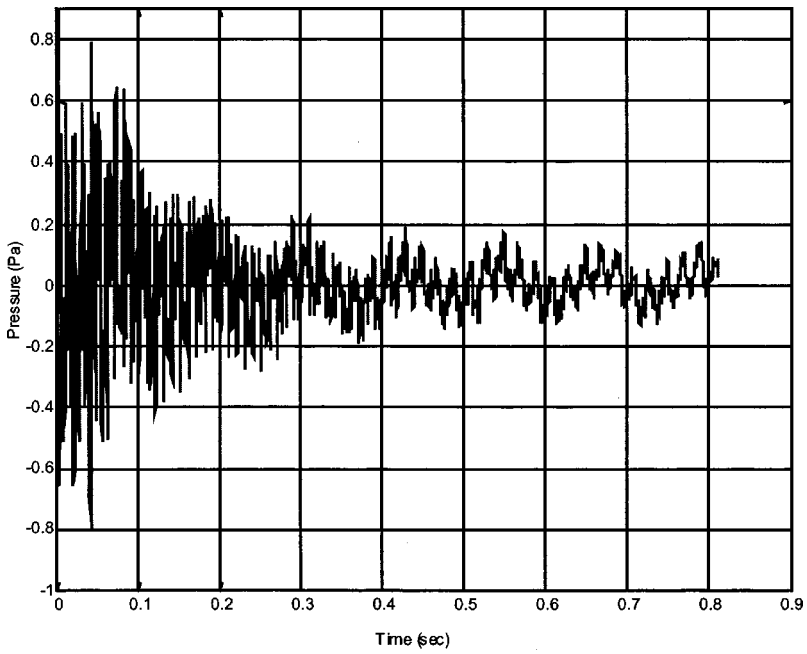

FIG. 10. Transient performance during reflection control for perfect absorption via integration method.

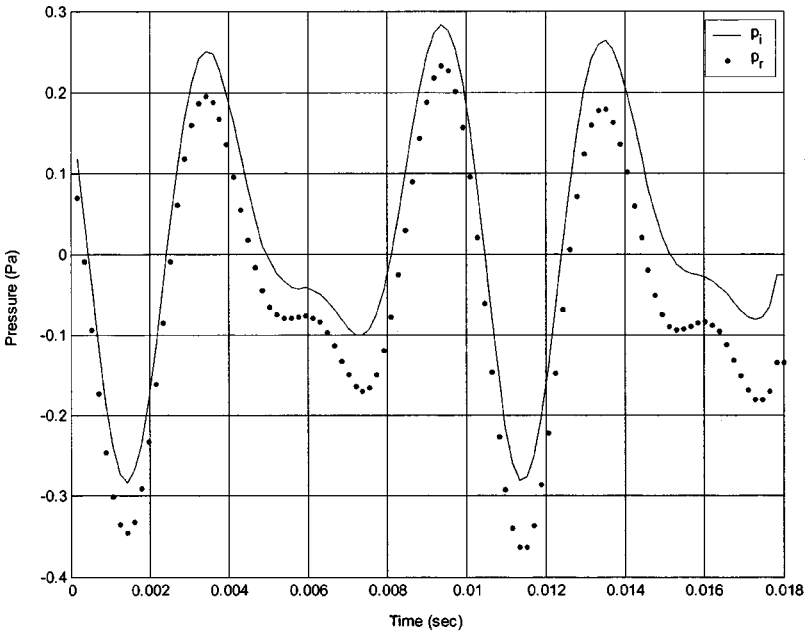

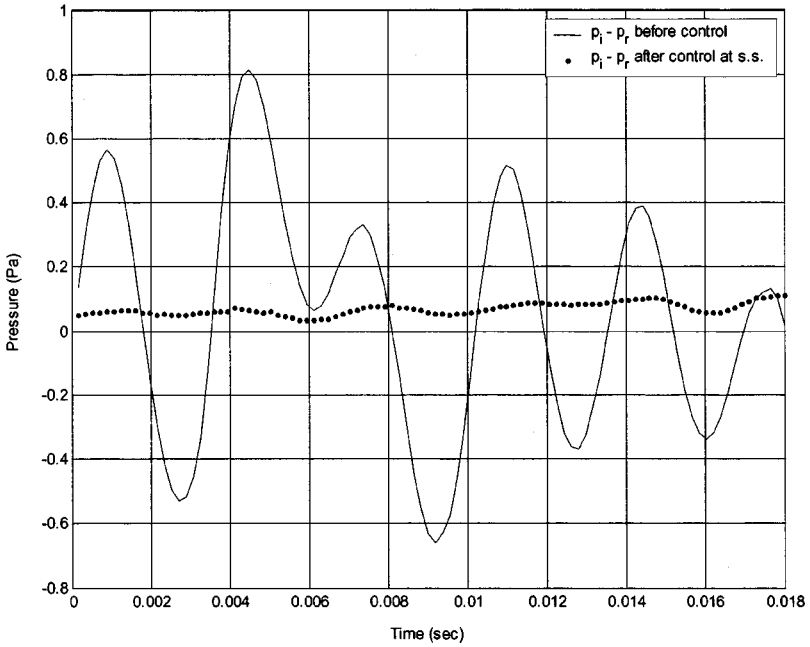

FIG. 11. Reflection control to achieve perfect reflection via integration method (primary noise consists of frequency components 200 and 300 Hz).

IV. ACTIVE CONTROL OF SOUND TRANSMISSION

A. Experimental setup

The experimental setup for sound transmission control is shown in Fig. 7. This is very similar to that used in active reflection control (see Fig. 4). A 2-m-long duct is used to isolate the environmental effects and ensure plane waves. The cross section of the duct is 17 by 17 cm. Thus, its cutoff frequency is about 1000 Hz. An additional third microphone is placed behind the panel speaker to measure the residual sound pressure that will be used for feedforward control. The objective of the sound blocker is to drive the pressure at this residual microphone to zero.

B. Method

Several different panel materials including poster board and glass can be used as speakers once equipped with the small electromagnetic motor actuators. Thus, a glass pane with an electromagnetic motor actuator functions effectively as a panel speaker. The advantages of a panel speaker are that it is thin, space saving, and inexpensive. The disadvantages are that it has uneven frequency response and is only able to provide limited power. Since the panel will not be boxed in an enclosure, it will generate and propagate sound from both sides of its surfaces. All these factors were carefully considered in the control design.

As can be seen in the experimental setup, the two mi-

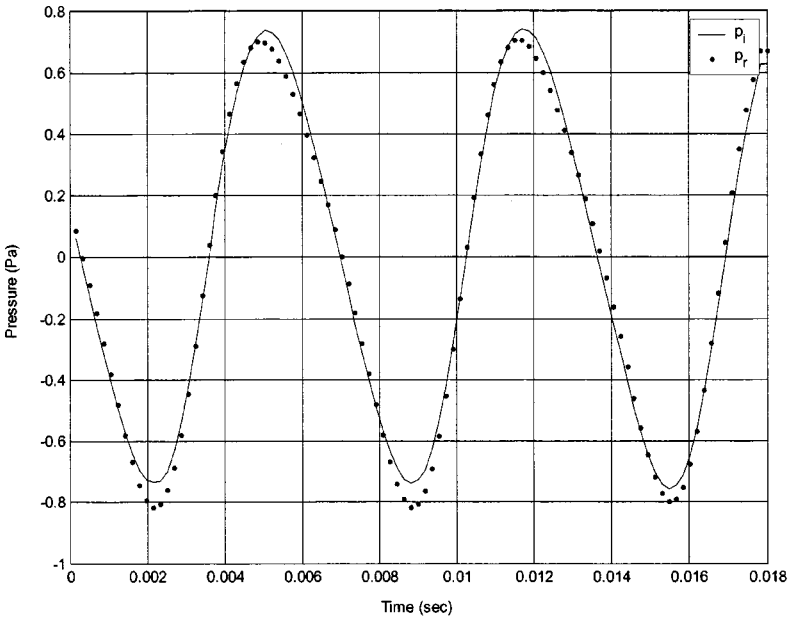

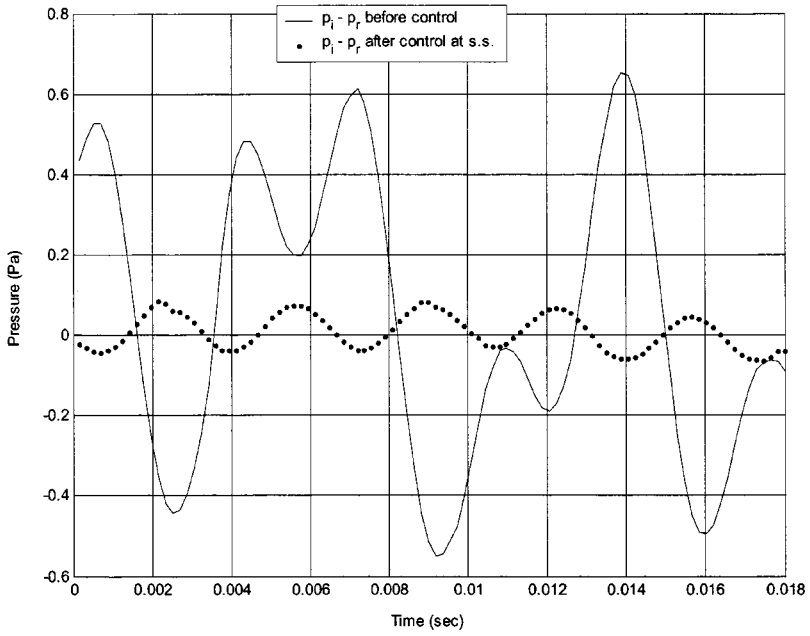

FIG. 12. Reflection control to achieve perfect reflection via integration method (primary noise consists of frequency components 150 and 300 Hz).

crophones in the path of the incident sound measure both the incident sound and the sound created from the panel itself. With the separation method, the incident wave is separated and used as a reference signal for feedforward control. The microphone at the other side of the panel measures the residual sound pressure which is then controlled to zero. A major distinguishing feature of the control system here is that a nonacoustic sensor is not needed for the reference signal. The incident sound is unaffected by the action of the speaker and hence we obtain a reference signal unaffected by the secondary source. All the signals from the microphones are sent to the PC via a data acquisition board. After wave separation, the reference signal is filtered by a FIR filter that represents the adaptive controller, the output signal is sent out to drive the panel speaker, and the signal from the error microphone is fed back to adapt the FIR filter coefficients.

The algorithm used to drive the residual sound pressure to zero is the same FXLMS algorithm described in Sec. III D.

V. EXPERIMENTAL RESULTS ON REFLECTION CONTROL

A. Integration method

1. Perfect absorber

A panel behaves as a perfect absorber if $p_r=0$, i.e., if there is no sound reflected back. To achieve perfect absorption using active control, the value of p_r is controlled to zero using feedforward control. In the integration method of reflected sound estimation, the residual error is p_r. The secondary path is $S(s)=P_r(s)-R(s)P_i(s)$, as explained in Sec. III B.

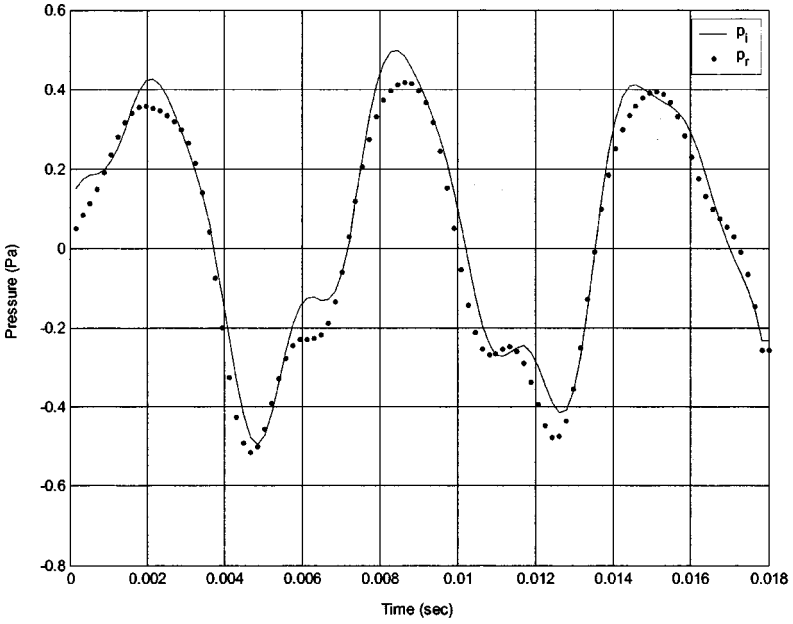

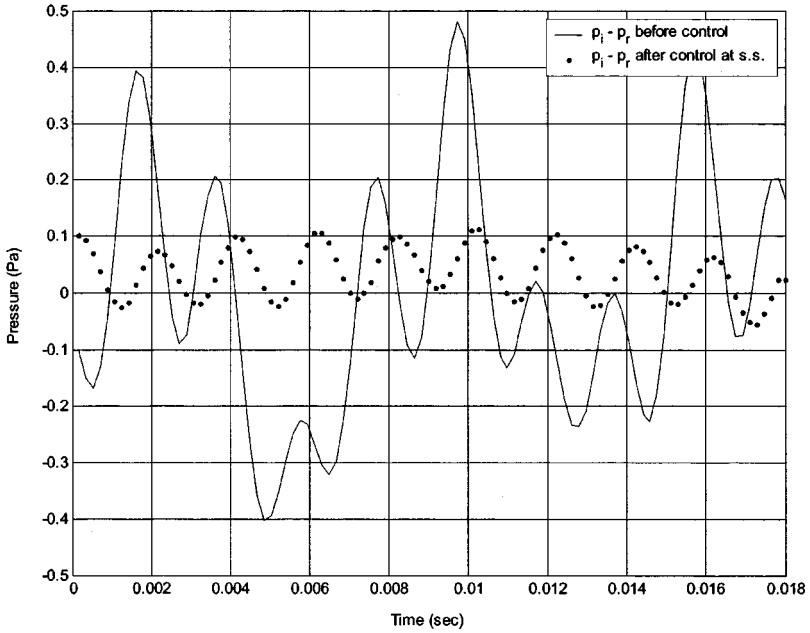

FIG. 13. Reflection control to achieve perfect reflection via integration method (primary noise consists of frequency components 150, 350, and 500 Hz).

Experimental results on reflection control to achieve perfect absorption are shown in Figs. 8, 9, and 10. The distance between the microphones in these experiments is 2.5 cm. Tonal noise is used since it is better illustrates reflection control, especially for cases where the desired reflection coefficient is nonzero. In the figures, the signals without any active control are compared with steady-state (s.s.) signals after control. The signals shown in the figures are the separated reflected waves in each case. In perfect absorption, there should be no reflection. The signals are measured indirectly via the PC. In Fig. 8 the primary noise consists of four frequency components (150, 200, 250, and 300 Hz), while in Fig. 9 the primary noise consists of two frequency components (100 and 300 Hz). As can be seen in the figures, there is a better than factor of 10 reduction in the reflected sound pressure. The transient performance of the controller is illustrated in Fig. 10. The control system has a time constant less than 0.5 s. The reflected sound pressure is seen to reach close to steady state in about 0.6 s.

2. Perfect reflector

A panel behaves as a perfect reflector if $p_r = p_i$, i.e., if all the incident sound is "reflected." To achieve perfect reflection, the reflected sound p_r is controlled to be equal to p_i using feedforward control. In the integration method, the secondary path is $S(s) = P_r(s) - R(s)P_i(s) = P_r(s) - P_i(s)$, as explained in Sec. III B. The residual error is just $p_r(t) - p_i(t)$.

The experimental performance of the reflection control system for perfect reflection is shown in Figs. 11, 12, 13, and 14. As can be seen, the control system ensures excellent

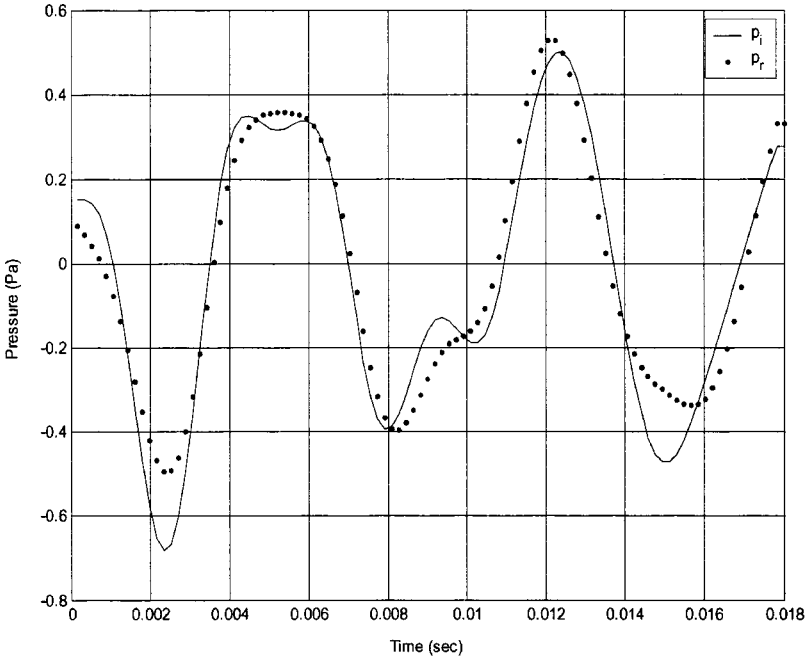

FIG. 14. Reflection control to achieve perfect reflection via integration method (primary noise consists of frequency components 150, 250, 350, and 400 Hz).

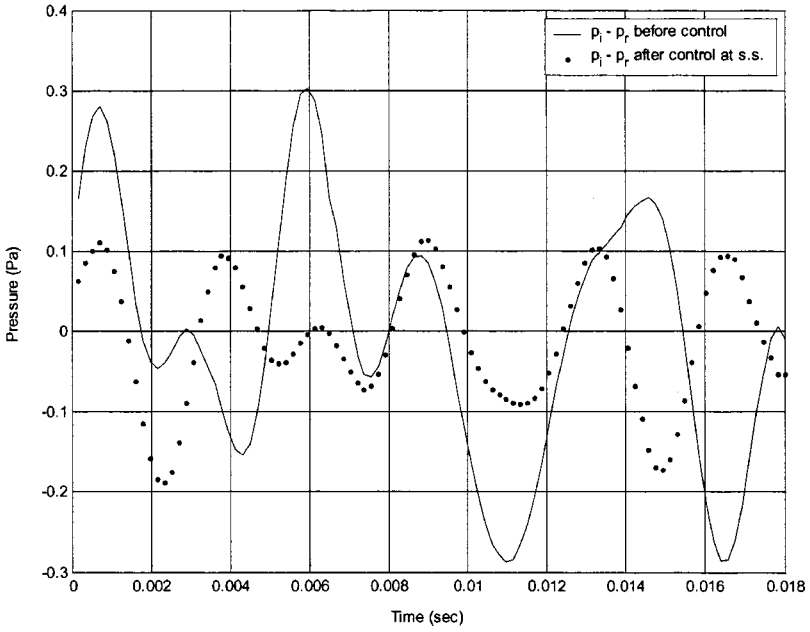

tracking between the incident sound and reflected sound waves. In every figure, there are two subfigures. The top subfigure shows the match between the incident wave and the reflected wave. The bottom subfigure shows the error between the incident and reflected waves to further illustrate the match. Multiple tones are used in each experiment. Different multiple tone combinations are shown in each figure. As can be seen in the figures, the performance tends to get worse when there are more frequencies contained in the primary noise.

3. Reflection coefficient greater than 1

In some applications such as in room acoustics, a coefficient greater than 1 may be desirable. In this section, experimental results on the case $R>1$ are shown to demonstrate the feasibility of achieving a reflection coefficient greater than 1 as long as the secondary source has adequate power. The integration method of wave separation is used.

Figure 15 shows the tonal case where the reflection coefficient is controlled to 1.2 for primary noise at a frequency of 200 Hz. As can be seen, the control system ensures good phase tracking between the incident sound and reflected sound waves with amplitude amplification. There are two subfigures in the figure—the left subfigure shows the match between the incident wave and the reflected wave and the right subfigure shows the error between the incident wave multiplied by 1.2 and the reflected wave to further illustrate the match. Reflection coefficient is controlled to 1.3 in Fig.

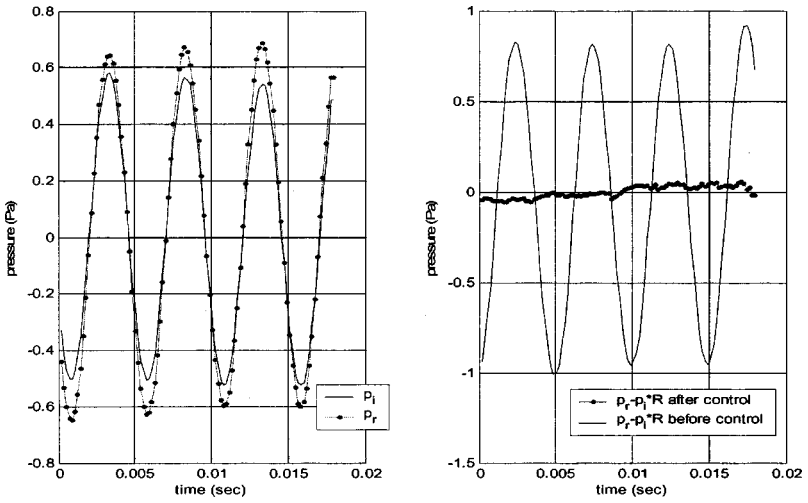

FIG. 15. Reflection control to achieve $R>1$ ($R=1.2$) via integration method (primary noise consists of frequency component 200 Hz).

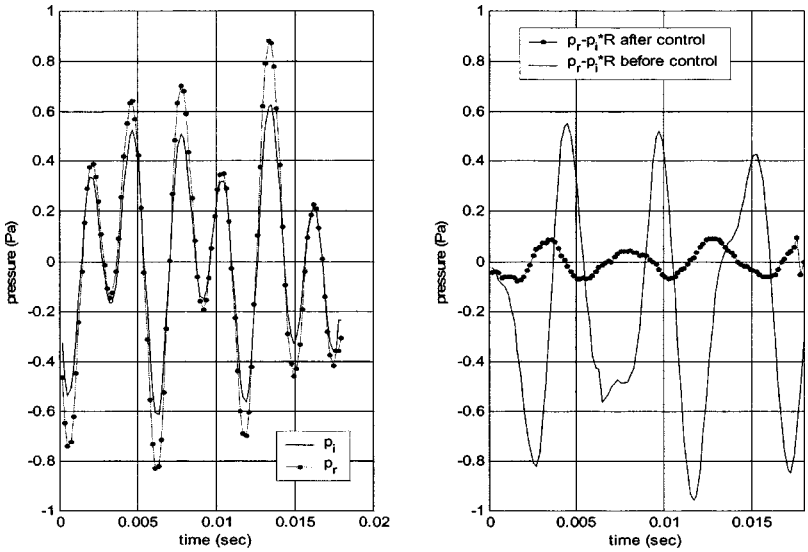

FIG. 16. Reflection control to achieve $R>1$ ($R=1.3$) via integration method (primary noise consists of frequency components 200 and 350 Hz).

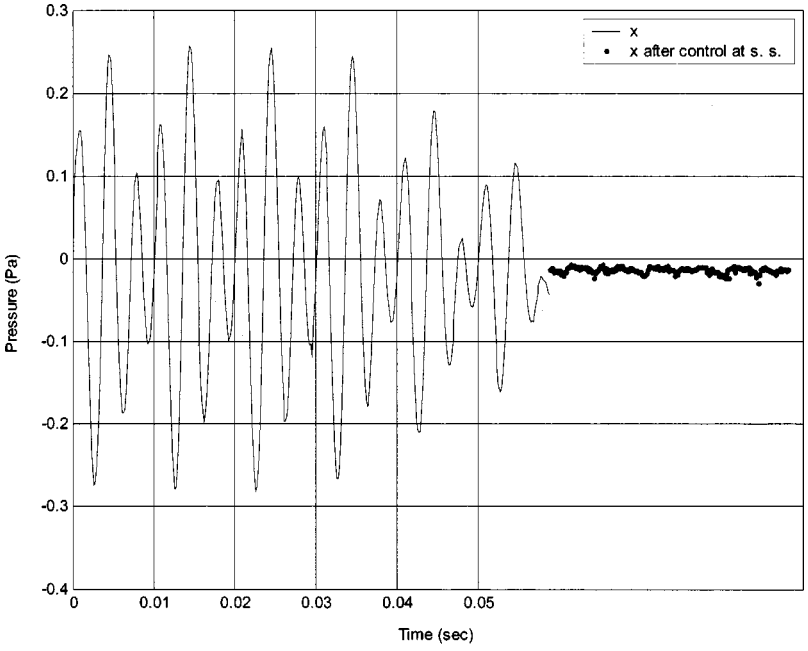

FIG. 17. Reflection control to achieve perfect absorption via delay method (primary noise consists of frequency components 200 and 300 Hz).

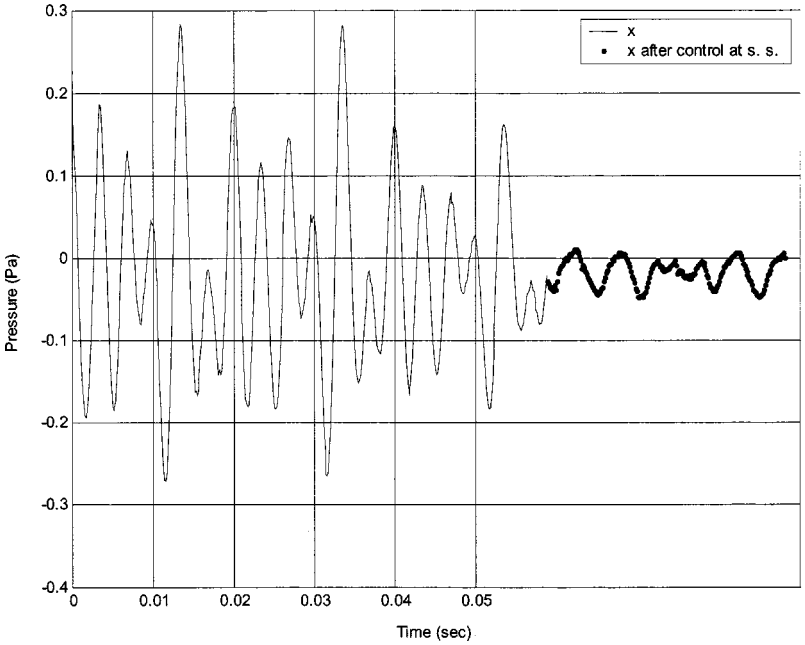

FIG. 18. Reflection control to achieve perfect absorption via delay method (primary noise consists of frequency components 150, 200, and 300 Hz).

16 with multiple tones at 200 and 350 Hz constituting the primary noise.

B. Delay method

1. Perfect absorber

In using the delay method for estimating the reflected and incident sound, the residual error signal and the secondary path change for the feedforward control system. The secondary path is $X(s)$, and the residual error is $x(t)$ as explained in Sec. III C. The objective here is to drive $x(t)$ to zero in order to get perfect absorption.

The experimental performance of the control system is shown in Figs. 17, 18 and 19. In the figures, the signals without any active control are compared with steady-state (s.s.) signals after control. The signals shown in the figures are "$x(t)$" in each case. In perfect absorption, $x(t)$ should be driven to zero. The signals are measured indirectly via the PC. In Fig. 17, the primary noise consists of two frequency components (200 and 300 Hz) while in Fig. 18, the primary noise consists of three frequency components (150, 200, and 300 Hz), and in Fig. 19, the primary noise consists of four frequency components (150, 200, 250, and 300 Hz). As can be seen in the figures, there is a better than factor of 10 reduction in the signal of "$x(t)$" in Fig. 17, and the performance gets slightly worse when the primary noise contains more frequencies.

2. Perfect reflector

For the perfect reflector case, again, the secondary path and the residual error are different compared to the integra-

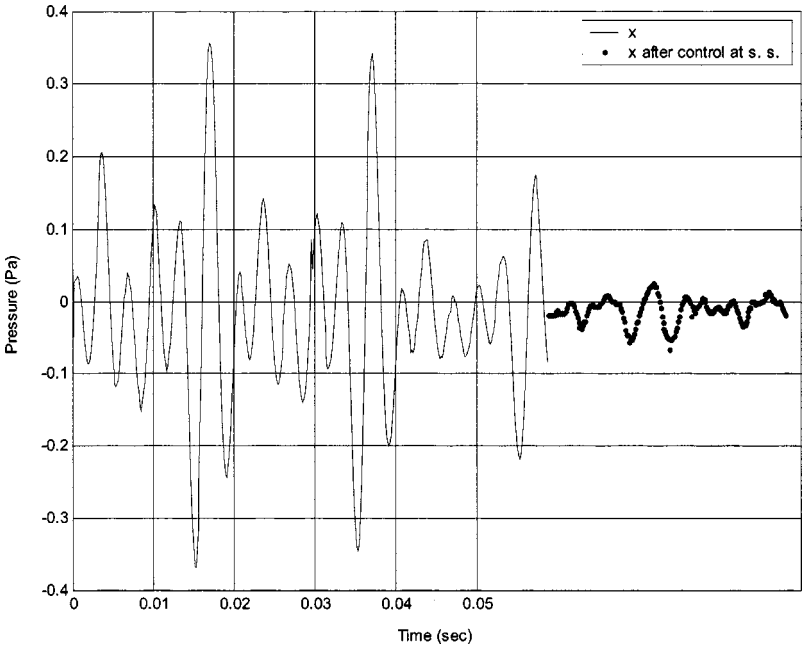

FIG. 19. Reflection control to achieve perfect absorption via delay method (primary noise consists of frequency components 150, 200, 250, and 300 Hz).

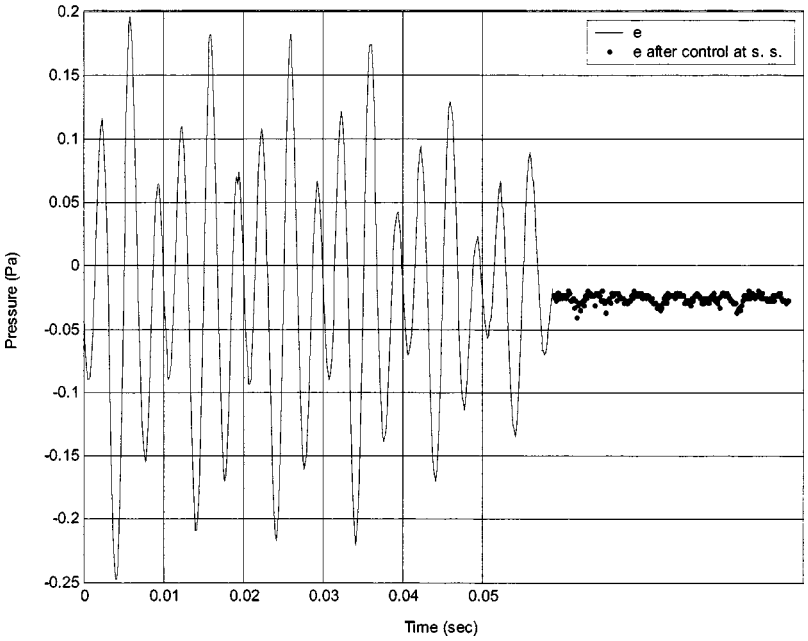

FIG. 20. Reflection control to achieve perfect reflection via delay method (primary noise consists of frequency components 200 and 300 Hz).

tion method. The secondary path is $X(s)-Y(s)e^{-(m+1)\tau s}$ and the residual error is $x(t)-y(t-(m+1)\tau)$. The objective here is to drive the conceptual residual error to zero in order to get perfect reflection.

The experimental performance of the system for achieving perfect reflection is shown in Figs. 20, 21, and 22. In the figures, the signals without any active control are compared with steady-state signals after control. The signals shown in the figures are the conceptual residual signal $x(t)-y(t-(m+1)\tau)$ in each case. In perfect reflection, the conceptual residual signal $x(t)-y(t-(m+1)\tau)$ should be driven to zero, i.e., $x(t)$ should match with a delay version of $y(t)$ in order to obtain $R=1$. The signals are measured indirectly via the PC. In Fig. 20, the primary noise consists of two frequency components (200 and 300 Hz) while in Fig. 21, the primary noise consists of three frequency components (150, 200, and 300 Hz), and in Fig. 22, the primary noise consists of four frequency components (150, 200, 250, and 300 Hz). As can be seen in the figures, there is a better than factor 10 of reduction in the signal of $x(t)-y(t-(m+1)\tau)$ in Fig. 20, and the performance gets slightly worse when the primary noise contains more frequencies.

C. Comparison between the two methods

The two methods for wave separation developed in this paper have their own advantages and disadvantages. The integration method requires the use of a high-pass filter to eliminate drift due to bias errors in acoustic pressure measurement. Also, the reflection coefficient calculated by the integration method has been found to have a dc error. However, this error remains constant and it is less than 1%. The

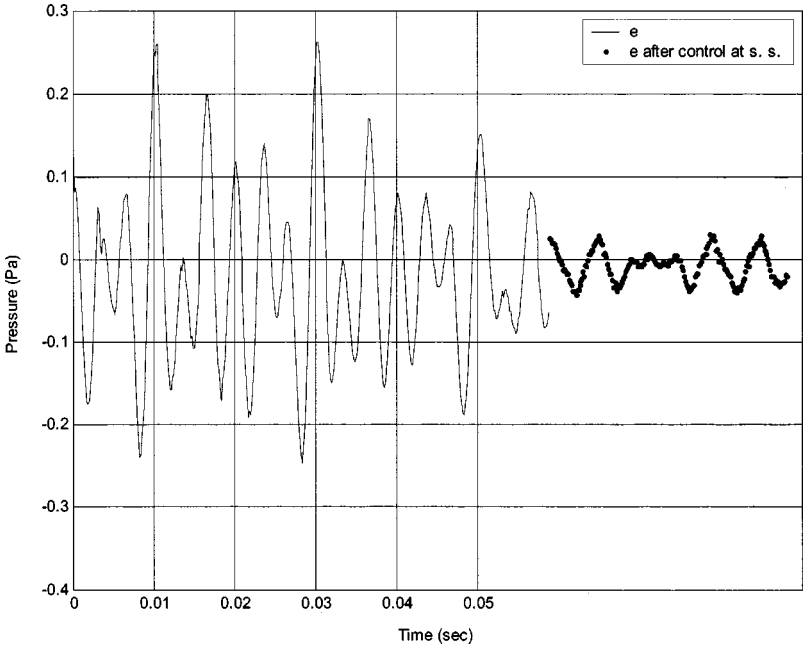

FIG. 21. Reflection control to achieve perfect reflection via delay method (primary noise consists of frequency components 150, 200, and 300 Hz).

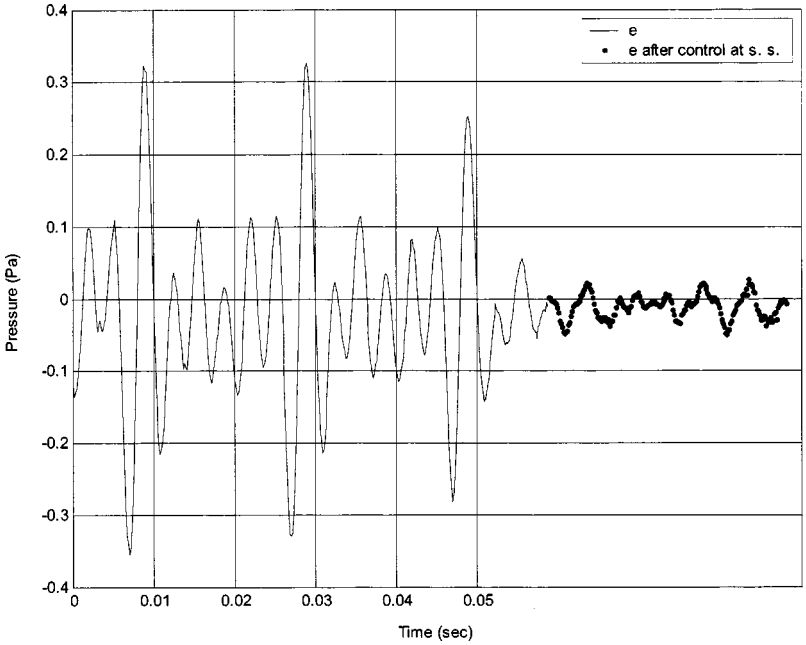

FIG. 22. Reflection control to achieve perfect reflection via delay method (primary noise consists of frequency components 150, 250, 200, and 300 Hz)

major disadvantage of the integration method is that it requires longer processing time due to the extra time needed for the integration as well as the high-pass filter operation. A big advantage of the integration method is that the incident wave is completely separated from the reflected wave. The incident wave can then serve as a reference signal for the FXLMS algorithm, and feedback effects from the secondary source can be successfully avoided. This advantage enables the method to also be used effectively in sound transmission control to obtain the reference signal.

From a faster processing time point of view, the delay method has an advantage. Only signals and their one-step delay versions are needed in this method. This speeds up the processing and a one-step delay is easy to implement in any DSP processor. The potential issues for the delay method that must be considered are that the magnitudes of x and y are small; thus, signal resolution is lost not only by the data-acquisition board but also during the DSP processing. Special care such as scaling may be needed in order to increase the signal-to-noise ratio. The largest disadvantage of the delay method is that both x and y contain information from both the incident wave and the reflected wave. The signal x cannot be used as a reference signal because it is not isolated from the actions of the secondary speaker. Unless a nonacoustic reference signal is available, the delay method is not suitable for broadband control. In this experiment, all the secondary path transfer functions were estimated off-line. As can be seen in Sec. III, for the case of perfect reflection control, the estimation of the secondary path transfer function for the delay method are more complicated than those for the integration method.

All the results shown in this section on reflection control

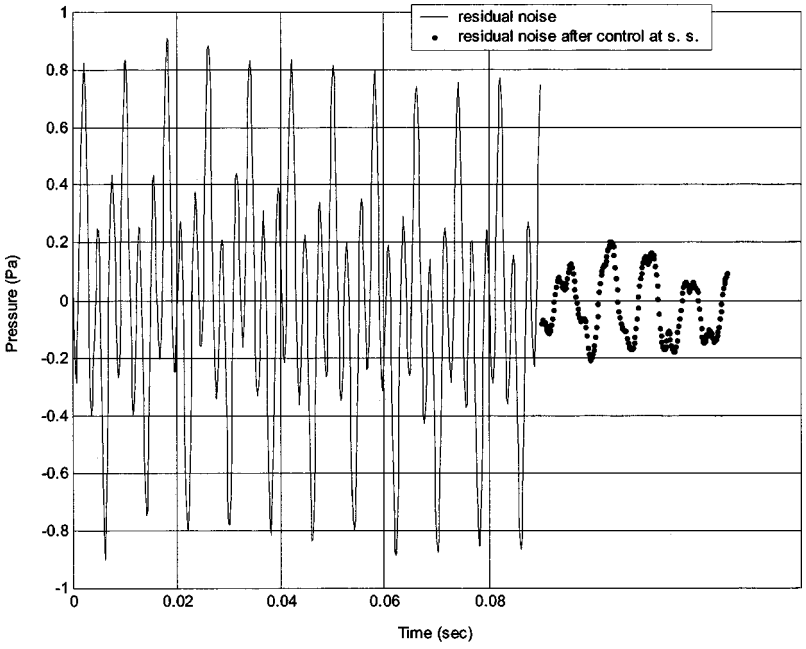

FIG. 23. Sound transmission control (primary noise consists of frequency components 125 and 375 Hz).

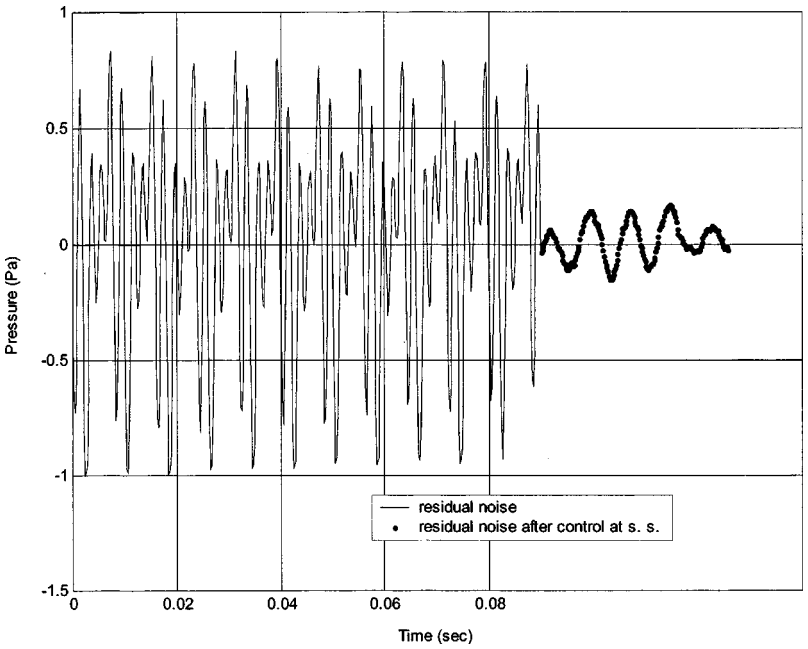

FIG. 24. Sound transmission control (primary noise consists of frequency components 125, 375, and 500 Hz).

are for harmonic noise. As can be seen in the figures, both methods work well. In the experiments, the sampling time while using the integration method was 180 microseconds while the sampling time via delay method was 140 microseconds. The time difference is expected to be larger if a microprocessor or DSP is used instead of a PC.

VI. EXPERIMENTAL RESULTS ON SOUND TRANSMISSION CONTROL

The experimental performance of the sound transmission controller described in Sec. III is shown in the figures below. In the experiment, a poster board is used as the panel. The secondary path transfer function is measured off-line. An order of 32 FIR filter is used to estimate this transfer function. Another order of 32 adaptive FIR filter is used for the FXLMS algorithm. The sampling time used is 180 microseconds.

Figures 23 and 24 show the performance of the transmission control system when the primary noise consists of discrete frequency components. Figures 25 and 26 show the performance when the primary noise consists of random noise bandlimited to frequencies below 800 Hz. In the figures, the signals without any active control are compared with steady-state signals after control. The signals shown in the figures are residual noise picked up by the third microphone positioned behind the panel in each case which should be driven to zero in order to block the sound transmission through the panel. In Fig. 23, the primary noise consists of two frequency components (125 and 375 Hz) while in Fig.

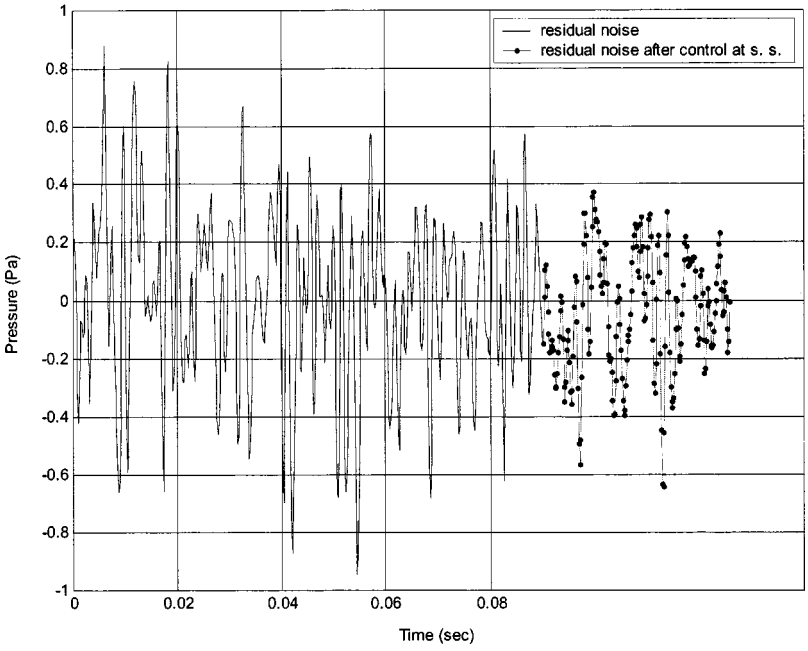

FIG. 25. Sound transmission control using a standard acoustic reference (primary noise is random containing frequency components up to 800 Hz).

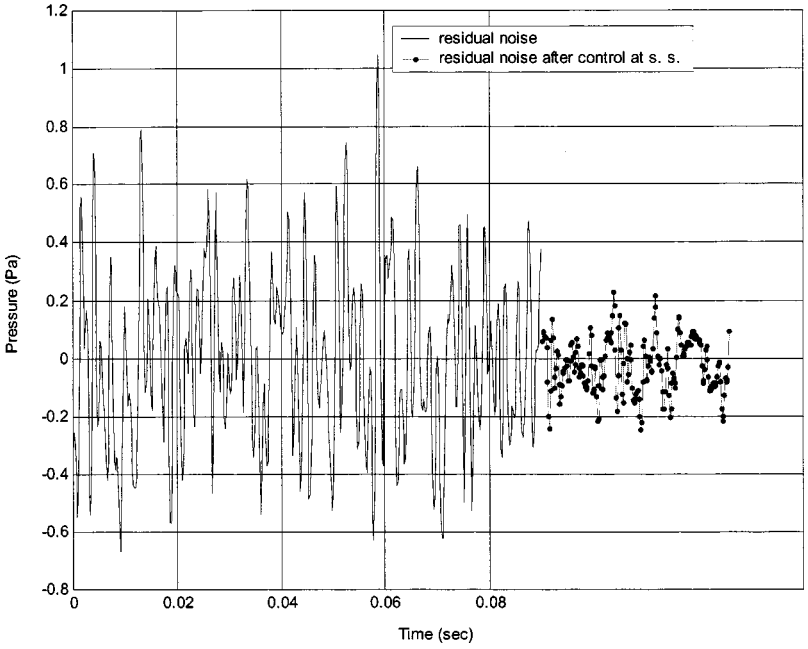

FIG. 26. Sound transmission using the separated incident sound as a reference (primary noise is random containing frequency components up to 800 Hz).

24, the primary noise consists of three frequency components (125, 375, and 500 Hz). As can be seen in the figures, there is a better than factor of 5 reduction in the residue noise for the case when the primary noise contains discrete frequency components, and the performance is worse when the primary noise contains random noise bandlimited to frequencies below 800 Hz.

In Fig. 25, a single standard microphone is used to pick up a signal which is then used as a reference. In Fig. 26, the wave separation method is used to separate the incident sound which is then used as the reference signal. As can be seen, the use of the incident sound as a reference provides significantly superior performance. This is also illustrated through a frequency response plot in Fig. 27. Figure 27 shows how the transmission control system provides significant noise attenuation over a broad range of frequencies. A comparison of performance obtained using just a single acoustic microphone to pick up the reference signal with the performance obtained when the incident sound is used as a reference is also shown. Clearly, the use of the incident sound as a reference provides superior performance. Overall, a performance of 10–15 dB is obtained over most of the frequency range via wave separation in Fig. 27.

A. Performance in terms of global sound attenuation

Previous results show that active sound transmission control at a point is possible. To make it practically useful, a global performance check is carried out too. The experimental setup is the same as in Fig. 7 except that an enclosure is connected to the duct. The enclosure is used to check the global noise reduction performance. The primary noise comes from the duct. It goes into the enclosure via the thin

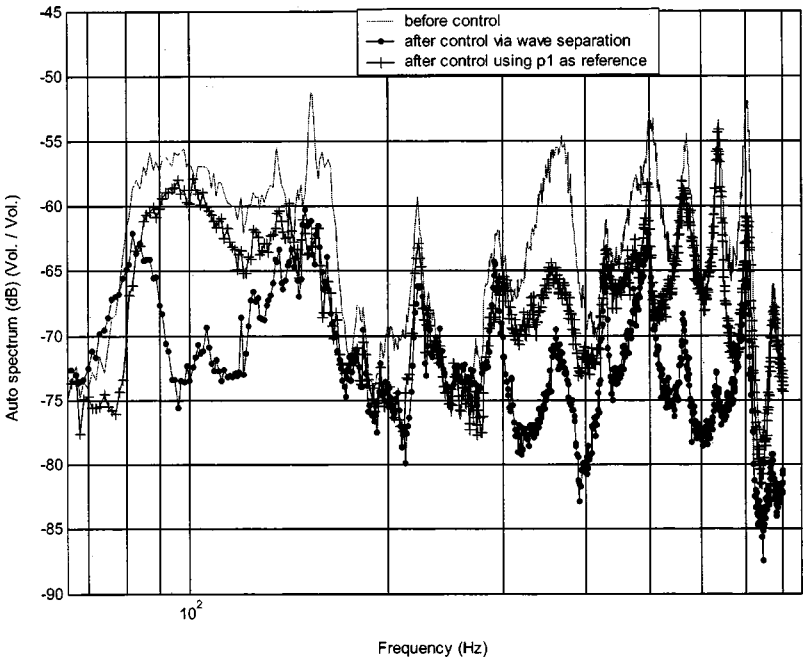

FIG. 27. Sound transmission control—frequency response (primary noise is random, containing frequency components up to 800 Hz).

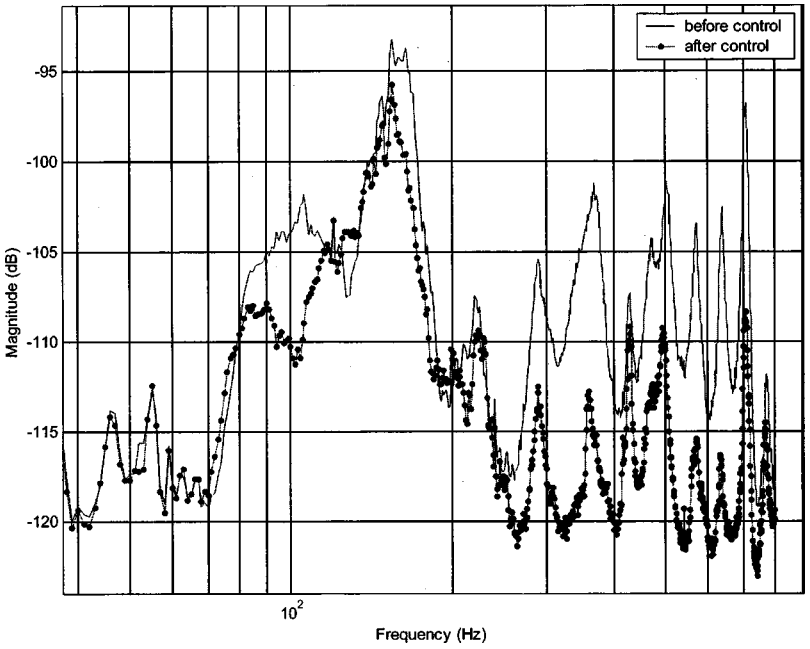

FIG. 28. Effect of the transmission controller on global sound in an enclosure.

panel. A cubic enclosure of size $0.4\times0.4\times0.4\ \mathrm{m}^3$ is considered. On the side of the enclosure that will be connected to the duct, a rectangular opening of the size of the duct is cut and a thin panel with an electromagnetic motor is mounted on this side of the enclosure. The primary noise is incident onto this thin panel. The panel is controlled so as to reduce noise transmission through the panel. Sound levels at different points inside the enclosure are then measured to evaluate if sound inside the entire enclosure is reduced by the use of this control system. Experimental results showed that the sound inside the enclosure was reduced everywhere. Figure 28 shows the sound pressure (averaged over 20 points) as a function of frequency before and after control. It shows that sound transmission is reduced at all frequencies by the control system. Figure 29 shows the performance at the error microphone. As noticed in the figures, there is coupling between the plate and the cavity. As shown in Fig. 29, the noise is dominated by an acoustic resonance at around 150 Hz. Altogether, measurements at 20 points were taken inside the enclosure. For every measurement, it was repeated (averaged) 50 times via the signal analyzer. No sound amplification at any frequency was found for every measurement, although the attenuation is not uniform throughout the enclosure.

VII. CONCLUSIONS

This paper explored the development of thin panels that could be controlled electronically so as to be either perfect reflectors or absorbers or acoustic transmission blockers. The

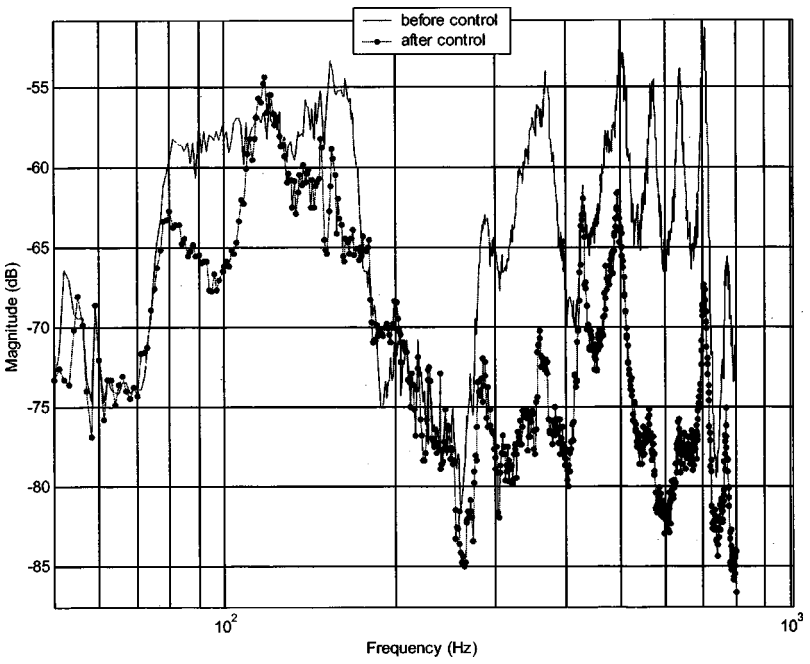

FIG. 29. Residual sound at the error microphone for the enclosure application.

panels were constructed using poster board and small rare-earth actuators. The development of the system was based on the use of a wave separation algorithm that separated incident sound from reflected sound. The reflected sound was then controlled to desired levels. The incident sound served an important purpose of providing an acoustic reference that is unaffected by the action of the control system speaker. The use of this incident signal reference also played a key role in the use of the panels as transmission blockers where the acoustic pressure behind the panel was driven to zero.

Detailed experimental results were presented showing the efficacy of the developed algorithms in achieving real-time control of reflection or transmission. The panels were able to effectively block transmission of broadband sound with the use of the incident wave playing a crucial role in allowing control without the use of a nonacoustic reference. The development of the panels is of practical importance with potential applications that include enclosures for noisy machinery, noise-absorbing wallpaper, the development of sound walls, and the development of noise-blocking glass windows. While the actuators will block light and are not transparent, they utilize rare-earth magnets and can be made with a diameter as small as 20 mm. These can be mounted near the corners of the window or hidden by patterned designs on the pane so as to be unobtrusive and therefore valuable for the glass windows application.

In the current research, only the normal incidence case has been investigated. When the incident angle is not normal, it is expected that the panel will continue to function well as long as the incident angle is not too oblique. The reflection coefficient at oblique incidence is given by

$$R = \frac{Z\cos(\theta) - Z_o}{Z\cos(\theta) + Z_o}, \tag{30}$$

where Z_o is the acoustic impedance of air, Z is the acoustic impedance at the panel surface, and θ is the angle of incidence. Thus, we can see that for small θ, the reflection coefficient is approximately equal to that at normal incidence.

In order to account for oblique incidence explicitly (if the angle of incidence were expected to be large), the relevant problem to be addressed is the development of the wave separation algorithm to reflect the change in incident angle. If the panel position is fixed and the incident angle is known, an extra microphone can be used to estimate the incident angle. If the incident angle is not known, an array of microphones around the panel would be needed for wave separation.

ACKNOWLEDGMENTS

This project was partially funded by Thermoking, Inc, Minneapolis, MN. The actuators for the panel speakers were provided by Kodel, Inc, Schaumburg, IL. The authors would like to express their appreciation to Steve Gleason and Jeff Berge from Thermoking and Mike Delazzer from Kodel.

Beranek, L. L. (**1954**). *Acoustics* (McGraw-Hill, New York), Chap. 2, pp. 16–46.

Chaplin, G. B. B. (**1977**). ''Active attenuation of recurring sound,'' U.S. Patent 4153815.

Furstoss, M., Thenail, D., and Galland, M. A. (**1997**). ''Surface impedance control for sound absorption: Direct and hybrid passive/active strategies,'' J. Sound Vib. **203**(2), 219–236.

Guicking, D., and Karcher, K. (**1984**). ''Active impedance control for one-dimensional sound,'' J. Vibr. Acoust. Stress Reliab. Des. **106**, 393–396.

Hansen, C. H. (**1991**). *Active Control of Noise and Vibration* (Department of Mechanical Engineering, University of Adelaide, South Australia), Chap. 1, Vol. 2.

Henrioulle, K., Desplentere, F., Hemschoote, D., and Sas, P. (**1999**). ''Design of an Active 1/4 Wavelength Resonance Absorber Using a Flat Loudspeaker,'' Active 99, pp. 1147–1158.

Kuo, S. M., and Morgan, D. R. (**1996**). *Active Noise Control Systems—Algorithms and DSP Implementations* (Wiley, New York), Chap. 1, pp. 1–16, Chap. 6, pp. 187–191, Chap. 3, 53–100.

Kuo, S. M., and Morgan, D. R. (**1999**). ''Active noise control: A tutorial review,'' Proc. IEEE **87**(6), 943–972.

Lacour, O., Galland, M. A., and Thenail, D. (**2000**). ''Preliminary experiments on noise reduction in cavities using active impedance changes,'' J. Sound Vib. **230**(1), 69–99.

Lueg, P. (**1936**). ''Processing of silencing sound oscillation,'' U.S. Patent 2043416, 9, June 1936.

Mehta, P. G., Zander, A. C., Patrick, W. P., and Zhang, Y. (**1998**). ''Active acoustic treatment (AAT)—a step toward a perfect sound absorber,'' in Proceedings of the American Control Conference, Philadelphia, PA, pp. 2611–2615.

Paurobally, R., Pan, J., and Bao, C. (**1999**). ''Feedback Control of Noise Transmission Through a Double-Panel Partition,'' Active 99, pp. 375–386.

Thenail, D., Galland, M., and Sunyach, M. (**1994**). ''Active enhancement of the absorbent properties of a porous material,'' Smart Mater. Struct. **3**, 18–25.

Thenail, D., Lacour, O., Galland, M. A., and Furstoss, M. (**1997**). ''The active control of wall impedance,'' Acustica **83**, 1039–1044.